

The Atmospheric Response to Realistic Arctic Sea Ice Anomalies in an AGCM. Part I: Winter.

MICHAEL A. ALEXANDER¹, UMA S. BHATT², JOHN E. WALSH³
MICHAEL S. TIMLIN³, JACK S. MILLER⁴, AND JAMES D. SCOTT¹

¹ NOAA-CIRES Climate Diagnostics Center, Boulder, Colorado

² International Arctic Research Center, University of Alaska Fairbanks, Fairbanks Alaska

³ Department of Atmospheric Sciences, University of Illinois at Urbana-Champaign, Urbana, Illinois

⁴ Institute of Northern Engineering, University of Alaska Fairbanks, Fairbanks Alaska

(submitted to Journal of Climate 2/03)

ABSTRACT

The influence of realistic Arctic sea ice anomalies on the atmosphere during winter is investigated with the Community Climate Model (CCM, version 3.6). Model experiments are performed for the winters with the most (1982-83) and least (1995-96) Arctic ice coverage during 1979-99, when ice concentration estimates were available from satellites. The experiments consist of 50-member ensembles: using large ensembles proved critical to obtaining reliable results.

The local response to ice anomalies over the subpolar seas of both the Atlantic and Pacific is robust and generally shallow with large upward surface heat fluxes ($> 100 \text{ Wm}^{-2}$), near-surface warming, enhanced precipitation, and below normal sea level pressure where sea ice receded, and the reverse where the ice expanded. The large-scale response to reduced (enhanced) ice extent to the east (west) of Greenland during 1982-83 resembles the negative phase of the Arctic Oscillation/North Atlantic Oscillation (AO/NAO) with a ridge over the poles and a trough at midlatitudes. The large-scale response was distinctly different in the Pacific, where ice anomalies in the Sea of Okhotsk generate a wave train that extends downstream over North America. Comparing the AGCM response to observations suggests that the feedback of the ice upon the atmospheric circulation is positive (negative) in the Pacific (Atlantic) sector. The magnitude of the wintertime response to ice extent anomalies is modest, on the order of 20 m at 500 mb. However, the 500 mb height anomalies roughly double in strength over much of the Arctic when the model is driven by ice concentration rather than ice extent anomalies. Furthermore, the NAO-like response increases linearly with the aerial extent of the Atlantic ice anomalies and thus could be quite large if the ice edge retreats as a result of global warming.

1. Introduction

Sea ice is a critical component of the climate system since it strongly influences albedo, surface turbulent heat fluxes, surface wind drag and upper ocean stratification. Thus, changes in Arctic sea ice strongly impact local climate variability and could potentially alter the global climate via changes in the thermohaline circulation and the location of storm tracks.

In addition to a large seasonal cycle, Arctic sea ice exhibits variability on subseasonal to decadal and longer

timescales (Walsh and Johnson 1979; Walsh and Chapman 1983; Mysak and Manak 1989; Fang and Wallace 1994; Parkinson et al. 1999; Polyakov and Johnson 2000; Serreze et al. 2000). Most studies have found that changes in sea ice concentration during winter primarily result from surface heat flux (thermodynamic) and wind stress (dynamic) forcing of the ice by the atmosphere (e.g. Agnew 1993; Fang and Wallace 1994, Proshutinsky and Johnson 1997). In the Atlantic, strengthening of the North Atlantic Oscillation (NAO, e.g. Hurrell et al. 2003) is associated with an intensification of the Icelandic low and advection of anomalously warm (cold) air to the east (west) of Greenland. As a result, ice extent increases in the Labrador Sea and decreases in the Greenland, Iceland, and Norwegian (GIN) seas (Chapman and Walsh, 1993), a pattern that exhibits both pronounced decadal variability and a long-term trend (Mysak et al. 1990; Slonosky et al. 1997; Deser et al.

Corresponding Author Address: Michael Alexander, NOAA CIRES Climate Diagnostics Center, R/CDC1, 325 Broadway, Boulder, CO 80305-3328.
Email: maa@cdc.noaa.gov

2000, 2002). In the Pacific, Overland and Pease (1982) presented evidence that the path of synoptic storms influences the sea ice edge in the Bering Sea. On a basin-wide scale, wind and heat flux anomalies associated with a wave train over the Pacific rim, which bears some resemblance to the “North Pacific Oscillation” (Rogers 1981), leads to anomalies of opposite sign in the Sea of Okhotsk and the Bering Sea (Cavaleri and Parkinson 1987; Fang and Wallace 1994).

One major exception to the paradigm of the atmosphere directly forcing ice variability occurs in the Greenland sea where the East Greenland Current transports ice southward through the Fram straight (Walsh and Chapman 1990), which can lead to large and long-lived anomalies in the North Atlantic (e.g. Dickson et al. 1988). The coherent variability in the atmosphere-ocean-ice system in the Arctic/North Atlantic has led to several hypotheses for decadal oscillations (Ikeda 1990; Mysak et al. 1990; Mysak and Venegas 1998; Ikeda et al. 2001; Goosse et al. 2002), which all require that sea ice anomalies have a pronounced impact on the atmosphere.

Some observational analyses also suggest that sea ice anomalies affect the overlying atmosphere. Deser et al. (2000) found that reductions in Greenland Sea ice cover and the associated anomalies in air-sea heat fluxes result in a northward shift of the local storm track, while Slonosky et al. (1997) found that reduced ice in the Greenland Sea during winter is associated with decreased sea level pressure (SLP) and 500mb heights and increased surface air temperature (SAT) in the following winter. Other observational studies suggest that sea ice changes influence the atmosphere (e.g. Walsh 1983; Honda et al. 1996); however, it is difficult to establish cause and effect relationship solely from data without confirmation by model experiments.

The number of atmospheric general circulation model (AGCM) simulations conducted with sea ice anomalies are quite limited, especially in relation to the number of model experiments performed with specified SST anomalies. While many AGCM simulations have been conducted with both observed SSTs and sea ice extent (e.g. Gates et al. 1999; Rodwell et al. 1999), analyses of these integrations have generally not focused on the role of varying sea ice on the atmosphere. In addition, several previous AGCM experiments have used sea ice boundary conditions that are extreme compared to recent observations. For example, in the modeling studies of Newson et al. (1973), Warshaw and Rapp (1973), and Royer et al. (1990) all of the sea ice was removed from the Northern Hemisphere, while Williams et al. (1974) and Raymo et al. (1990) greatly reduced sea ice extent to represent paleoclimatic conditions. In these experiments, the reduction or elimination of sea ice led to an increase in SAT and reduced SLP over the Arctic, and a tendency for weaker midlatitude westerly winds.

Herman and Johnson (1978) were the first to examine the atmospheric circulation changes associated with the ice boundary conditions based on the present climate.

In their perpetual January AGCM simulations, Arctic sea ice extent was specified to be either in a maximum or minimum state at all longitudes, an envelope of extreme ice conditions, since the observed ice margin does not vary synchronously in all regions. Herman and Johnson found a significant response to the ice edge difference (maximum-minimum) in SLP, 700 mb temperature and 300 mb heights over the Arctic and North Atlantic and Pacific Oceans. They noted that the full atmospheric response could not be explained by local thermodynamics, suggesting that dynamical processes were important for the far field anomalies.

Murray and Simmonds (1995) and Simmonds and Budd (1991) examined the simulated atmospheric response to idealized specifications of sea ice fraction (concentration) in the Northern and Southern Hemispheres, respectively. In these perpetual winter experiments the ice edge remained constant, but the amount of open water was set to a fixed value in each square containing ice. They found that decreasing sea ice concentrations lead to a local monotonic but nonlinear increase in SAT and a weakening of the midlatitude westerlies. Less ice also resulted in a significant decrease in the speeds and intensities of storms poleward of 45°N, but little change in path of the storms. Parkinson et al. (2001) conducted AGCM experiments where the ice concentration was increased or decreased by a fixed amount in each grid square to quantify how errors in specification of ice fraction might influence the atmosphere. Changes in ice concentration influenced global SAT throughout the year but was greatest in fall and winter and in regions directly above where the ice concentration changed. In contrast to Murray and Simmonds (1995), Parkinson et al. found that SAT increased linearly as the ice concentration decreased.

Honda et al. (1999) examined the atmospheric response to maximum and minimum ice extent in the sea of Okhotsk, where the difference between the two ice states was specified to be approximately twice as large as what has been observed. The model produced a very large response both locally, and downstream over the Bering Sea, Alaska and North America. Wave activity diagnostics indicated that the remote response is a stationary Rossby wavetrain generated by surface heat flux anomalies associated with changes in ice extent. The difference between the two model experiments resembles the observed composite based on differences in ice concentration in the sea of Okhotsk.

Recently, in a two part study Magnusdottir, Deser and Saravanan, and Deser, Magnusdottir, Saravanan and Phillips (2003, MDS/DMSF from hereon) examined the atmospheric response to sea ice as well as SST anomalies in the North Atlantic in the National Center for Atmospheric Research (NCAR) Community Climate Model 3 (CCM3). The anomaly patterns used as boundary conditions in the CCM were derived from the observed trends during the past 40 years, although the magnitude of the anomalies was substantially amplified and the trend was treated as a perturbation that varied

with the seasonal cycle but did not change from one year to the next. In the sea ice experiment, the mean winter-time response was strong and resembled the NAO, with anomalies of one sign over the Arctic and opposite sign over the North Atlantic. However, the response was generally opposite to the observed atmospheric trend, suggesting a negative ice-atmosphere feedback.

While the aforementioned AGCM experiments indicated that changes in sea ice influence the atmosphere, they all used somewhat idealized ice configurations, and most employed models with relatively coarse horizontal resolution ($\sim 5^\circ \times 5^\circ$). Coarse resolution influences both how the boundary conditions are specified and how the atmosphere responds to those anomalies. Most previous AGCM studies also used a limited number of model realizations. Given the modest signal to noise ratio of the atmospheric response to boundary forcing, having a large ensemble and/or long integrations is critical to obtaining robust results (e.g. Robertson et al. 2000, Sardeshmukh et al. 2000). Here, we use large ensembles of CCM simulations forced with observed Arctic sea ice conditions during the winter periods with maximum and minimum ice coverage to examine how realistic sea ice variability influences the atmospheric circulation. Specific questions to be addressed include: by what dynamic and thermodynamic processes do sea ice anomalies influence the local and far field atmospheric circulation? Does the atmospheric response differ to anomalies in ice concentration versus ice extent? Do the characteristics of the response differ in winter and summer? Here we examine the winter response; the summer response will be presented in a companion paper by Bhatt et al. (2003).

2. Model Experiments

a. Experiment design and boundary conditions

Given the complicated nature of ocean-ice-atmosphere interactions and the difficulty in simulating Arctic sea ice concentration and thickness in coupled models (Weatherly et al. 1998, Bitz et al. 2002) we focus on how sea ice influences the atmosphere using AGCM simulations. Boundary conditions for the simulations were derived from ice concentration values in the Hadley Center's Ice SST dataset (HadISST version 1.1 - Rayner et al. 2000) during 1979-99, the period when continuous passive microwave measurements were available from satellite. We focus on the winters of 1982-83 and 1995-96 since they contained the maximum and minimum sea ice cover over the entire Arctic from November to March during the 1979-99 period. Three model experiments have been performed in which Arctic sea ice varies according to observations:

- Ice extent varies over the winter of 1982-83 (Win83e)
- Ice extent varies over the winter of 1995-96 (Win96e)

- Ice concentration varies over the winter of 1995-96 (Win96c),

where the experiments are designated, in parentheses above, by the season, year and ice configuration. We also performed an extended (55 year) control simulation in which

- Ice extent repeats the same seasonal cycle each year based on the average of the 1979-99 period (Cntle).

As a first step in creating the daily boundary conditions, the observed monthly mean values were interpolated to the model grid using bilinear interpolation over the open ocean and averaging of nearby grid values in coastal regions. In all experiments, the Arctic sea ice is specified to be 2.5 m thick; to isolate the influence of Arctic sea ice, global SSTs and sea ice in the Southern Hemisphere (specified to be 1 m thick) evolve according to the mean seasonal cycle in all of the experiments. In regions where the ice extent retracted compared to normal the exposed ocean was set to the climatological SST; when the ice was more expansive than normal, SSTs were blended from -1.8°C (the temperature at which there is 100% ice cover) at the ice edge to climatological values two grid boxes seaward from the ice. In the extent experiments, the monthly Arctic sea ice values were specified to cover 100% of the grid square if the observed monthly averaged concentration exceeded 15%, otherwise the grid square was set to be ice free.

In order to obtain daily boundary condition, the monthly mean ice and SST values were set to the middle of the month and then linearly interpolated in time in both the extent and concentration simulations. As a result, the transition from no ice to complete ice cover in a grid square is not instantaneous in the extent simulations, instead the amount of ice linearly increases (decreases) from 0% to 100% within the 30-day period when ice forms (melts). While this provides for a smooth transition of the ice edge in space and time, and is probably more realistic than an instantaneous transition, it also introduces fractional ice cover into the extent experiments.

The model boundary conditions and model response are shown on a monthly basis in (Scott et al. 2003)¹. The boundary forcing for January of the Win83e experiment is shown in Fig. 1 (the boundary conditions in the Win96 experiments are shown in Fig. 12 and discussed in section 3.c). Even though there are sizeable areas with less ice than normal, the winter of 1982-83 had the overall maximum ice area since the regions with increased ice were further south and thus encompassed greater area in terms of square kilometers. In the Atlantic, there is more ice relative to climatology in the Labrador sea and less in the Greenland, Iceland and Norwegian (GIN) Seas, while in the Pacific there is

1. Various monthly fields from these experiments and figures relevant to the paper which otherwise would not be shown are presented at <http://www.cdc.noaa.gov/~jds/Ice>.

Jan 1983 Ice Extent Anom

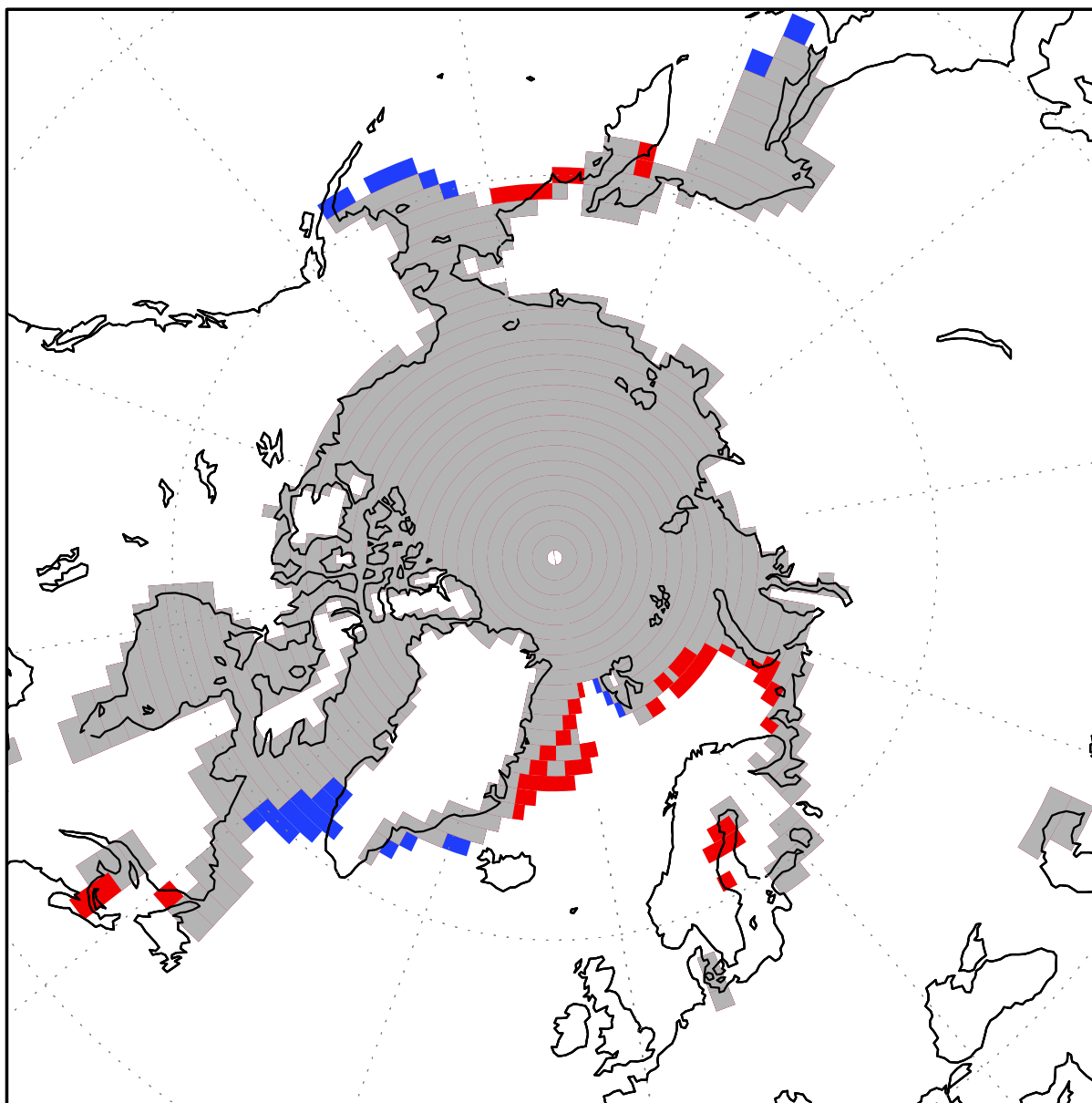


Fig. 1. Sea ice boundary conditions during January 1983 in the winter 1982-83 extent (Win83e) experiment. Gray indicates areas with climatological sea ice and blue (red) indicates grid squares where the ice edge has expanded (retreated) relative to climatology. Thus, the gray plus blue areas indicate the full ice extent in the Win83e experiment. Grid squares are set to be ice covered when the ice concentration, derived from the HadISST data set, exceeds 15%.

more ice in the southern Sea of Okhotsk and in eastern Bering Sea and less ice on either side of the Kamchatka Peninsula. This pattern, which persists through most of the winter, closely resembles the leading EOF of sea ice over the Northern Hemisphere (Deser et al. 2000).

b. AGCM

The CCM (version 3.6), the AGCM used in this study, has 18 vertical levels and a horizontal spectral resolution of T42, which is approximately 2.8° latitude by 2.8° lon-

gitude. Kiehl et al. (1998) described the model physics, while Hack et al. (1998) and Hurrell et al. (1998) examined the model's climate. While the model has some deficiencies over the Arctic, e.g. it's colder and wetter than observed (which also occurs in most other AGCMs [Randall et al. 1998]), many aspects of the earth's climate are well simulated.

c. Simulations: initial conditions, duration and ensemble size

The Win83e and Win95c&e experiments each consist of an ensemble of **50** CCM3 simulations that extend from October through the following April. Initializing the integrations in October allows time for the model to spin-up prior to December-January-February (DJF), the period used in most of our analyses. The boundary conditions evolve identically in each simulation within the ensemble but the simulations are initialized with different atmospheric states chosen from the last 50 years of the 55-year Cntle integration.

We anticipate that a large ensemble is necessary since most previous AGCM experiments indicate a modest atmospheric response to realistic midlatitude SST anomalies relative to the background climate variability. Student's t-test indicates a significant shift of the mean at the 95% confidence level requires that:

$$N < \frac{8}{(x'/\sigma)^2}$$

(e.g. see Sardeshmukh et al. 2000), where here N is the

number of simulations, x' the mean model response and σ the standard deviation of internal atmospheric variability. Given that the winter-to-winter 500 mb height σ ranges from 40-60 m over much of the Arctic and Northern Hemisphere Oceans in the CCM3 control integration, a mean response of 25 m at 500 mb over DJF would require roughly 20-45 ensemble members to be significant depending on the location of the grid point.

3. Results

The atmospheric response, defined by the ensemble average of the simulations within a given experiment minus the long term mean from the control, varies over time due to the evolution of the boundary conditions, the seasonal cycle of the climatic state and intersample variability. Here we focus on the results in the Atlantic and Pacific sectors during DJF, the atmospheric response for all months is presented in Scott et al. (2003).

a) Atlantic Sector: Win83e experiment

The change in the location of the ice edge (Fig. 1)

Win83–CNTL Qnet upwards DJF

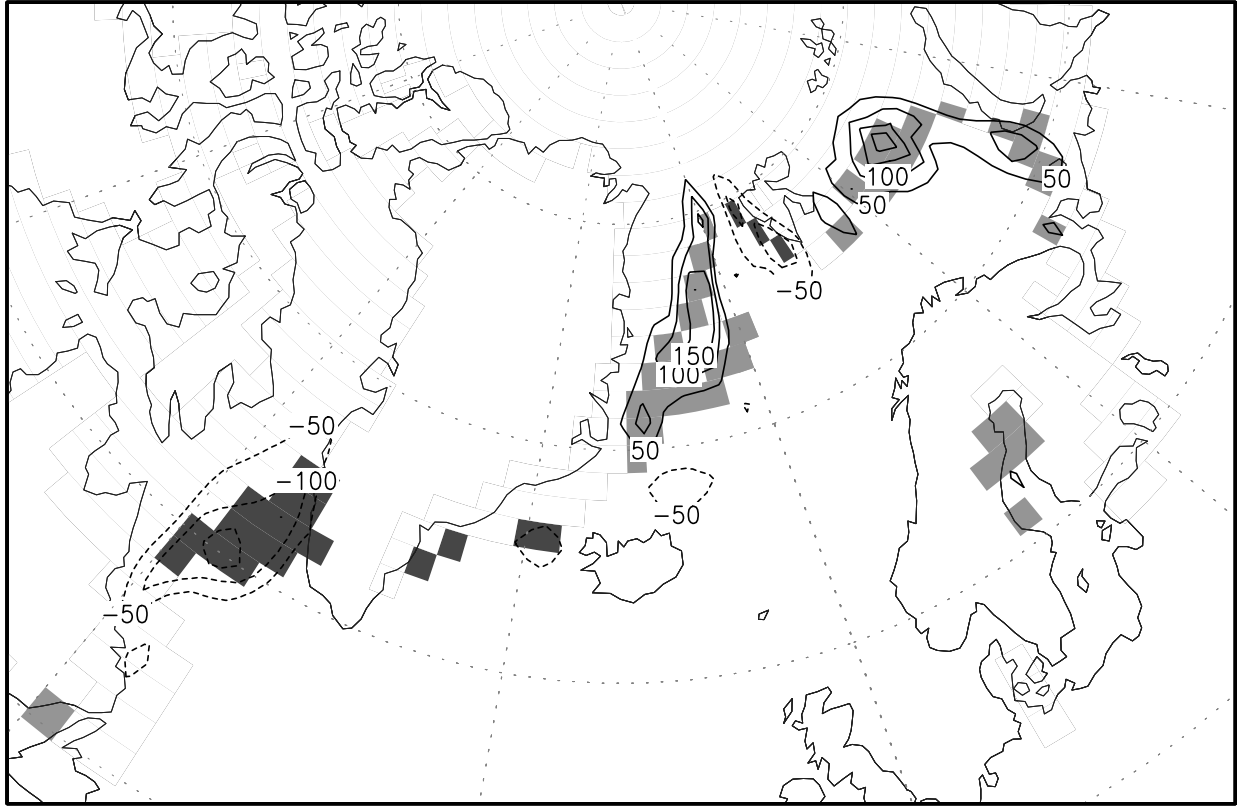


Fig. 2. Win83e net upward heat flux anomalies over the North Atlantic during December-January-February (DJF) of 1982-83 (contoured: interval of 50 W m^{-2} ; negative values dashed, zero contour omitted). The anomalies are defined as the ensemble mean of the 50 Win83e simulations minus the long-term mean of the 55-year control (Cntle) integration. The light (dark) shading indicates grid squares with less (more) ice in Win83e than in Cntle during January 1983; only one month is shown since its unclear how to average a binary quantity like ice extent when it varies over a season.

leads to intense surface heat flux anomalies (ensemble mean of the 50 Win83e simulations minus the long-term average from the Cntle experiment) in the North Atlantic sector (Fig. 2). Where the ice edge retreats, such as in the western Greenland Sea and Barents Sea, there are large net upward heat flux anomalies ($> 150 \text{ W m}^{-2}$); likewise negative heat flux anomalies occur where the ice expands, including the Davis Strait and to the west

of Svalbard. The flux anomalies are of much smaller spatial scale but of much larger magnitude than those associated with midlatitude SSTs. The net flux anomalies are due to the sensible, latent and longwave fluxes, where the sensible heat flux anomalies are approximately twice (quadruple) the latent (longwave) anomalies; the solar anomalies are negligible due to the limited amount of sunlight in the Arctic during winter.

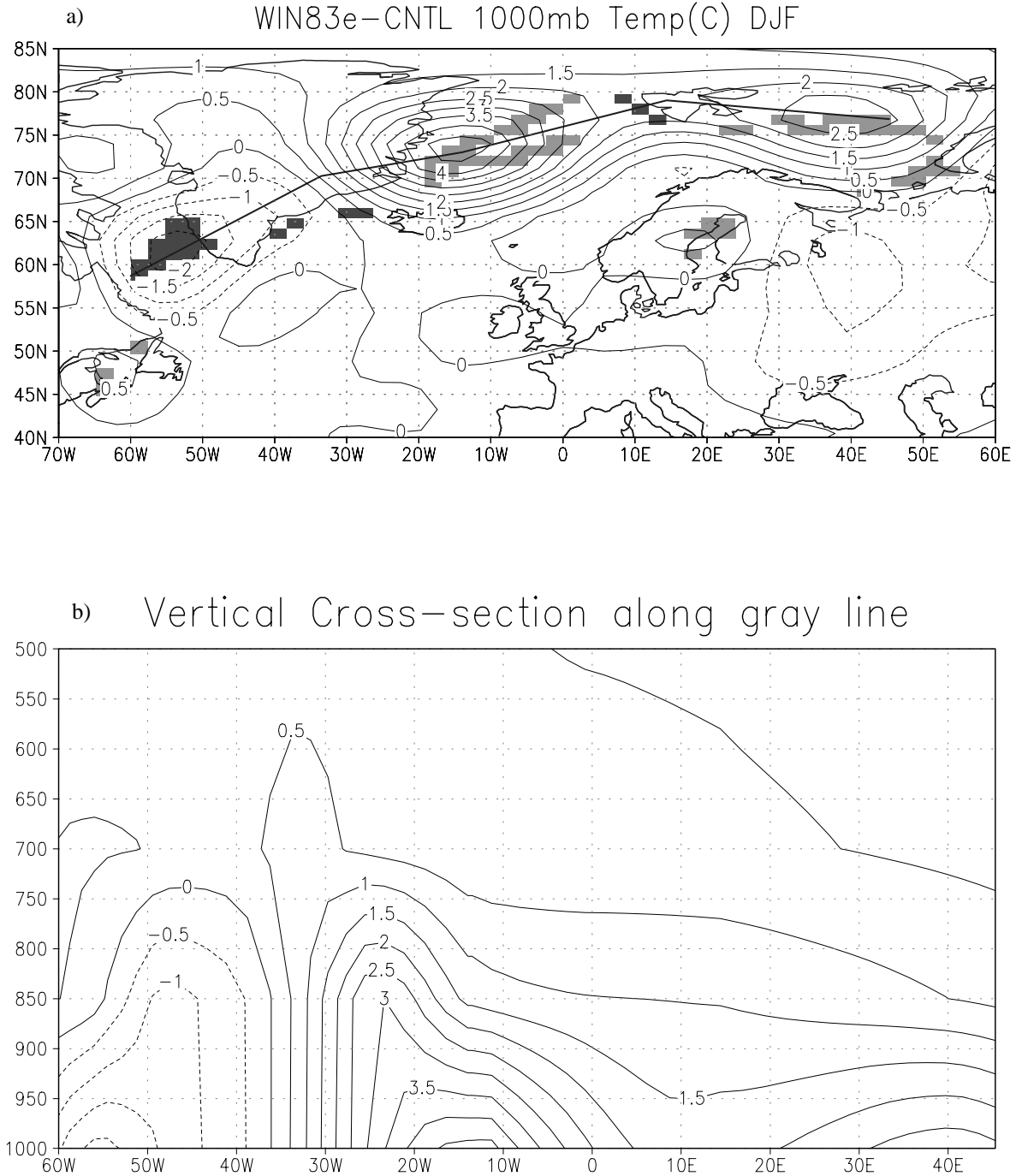
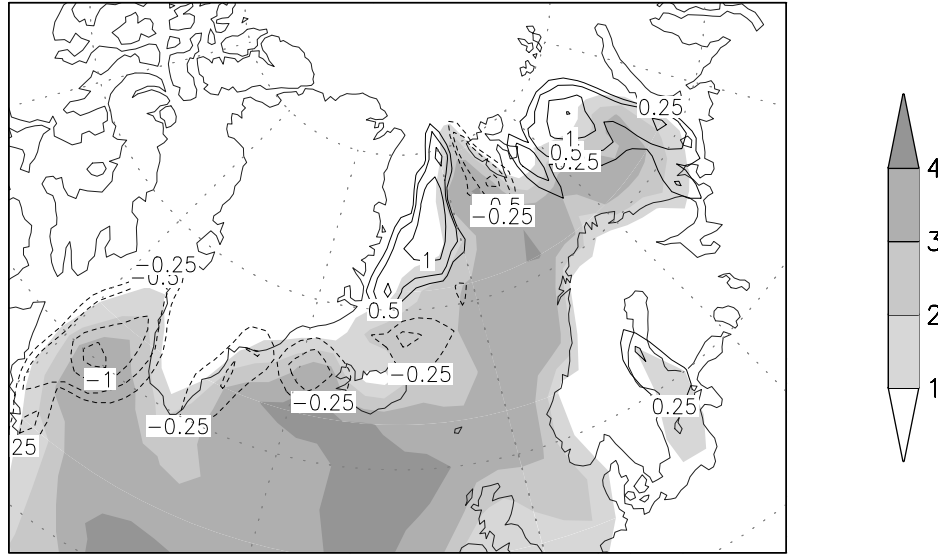


Fig. 3. Win83e temperature anomalies during DJF a) at the 1000 mb level (b) as a vertical cross-section along the transect line shown in (a) (contoured: interval 0.5°C ; negative contours dashed). As in Fig. 2, the light (dark) shading indicates grid squares with less (more) ice in Win83e than in Cntle during January 1983

WIN83e Anomalies (contour) CNTL (shaded)

a) Evaporation (mm/day)



b) Precipitation (mm/day)

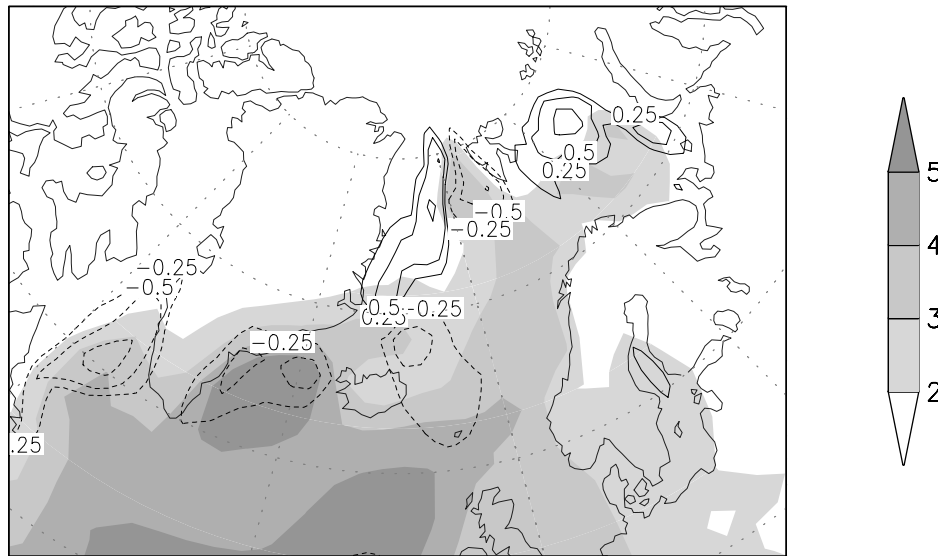


Fig.4. Win83e (a) evaporation and (b) precipitation anomalies (contours) and the long-term mean from the Cntle simulation (shading) during DJF. The contour interval is 0.25 mm day^{-1} , where the zero line is omitted; the shading interval is 1 mm day^{-1} .

The SAT anomalies (Fig. 3a) are positive above the reduced ice cover, collocated with anomalous upward heat fluxes, in the GIN and Barents Seas and are negative over the enhanced ice cover in the Labrador Sea. The ice and temperature anomalies are nearly collocated

indicating that advection has a modest influence on the thermal response far from the initial source of the anomalies. However, the passage of storms mixes the flux-driven thermal anomalies within a few hundred kilometers of the ice edge changes. In addition, the large-scale

atmospheric response has some influence on the anomalous SAT field, through the advection of temperature anomalies by the mean circulation and by the anomalous advection across the mean temperature gradient. For example, advection by the mean flow transports the anomalously warm air from the Greenland Sea south towards Iceland and from the Barents Sea towards the east Greenland Sea. The latter leads to the surprising result of positive temperature anomalies above increased ice cover along the west coast of Spitsbergen ($\sim 77^\circ\text{N}$, 10°E ; Scott et al. 2003, Fig. 1). Southerly wind anomalies over the strong mean meridional temperature gradient in the region 65°N – 80°N , 10°E – 30°W (Scott et al. 2003, Fig. 2) contributes to the anomalously warm air over the Greenland Sea seen in Fig. 3. Indeed, the magnitude of the SAT anomalies are approximately twice as large over the Greenland Sea compared to the anomalies over the Labrador and Barents Seas, even though the magnitude of the surface flux anomalies (Fig. 2) and the latent heating associated with precipitation (Fig. 4) are of similar magnitude over the three regions.

The atmospheric response to the ice edge changes is quite shallow (Fig. 3b). In the Barents and Labrador Seas the temperature anomalies decay from $\sim 2^\circ\text{C}$ at 1000 mb to near zero by 700 mb, while over Greenland Sea the response decreases from 4°C at 1000 mb to 0.5°C by 700 mb. The temperature anomalies extend slightly farther up into the atmosphere from 28°W to 35°W over Greenland, perhaps due to interactions between the steep topography and the circulation anomalies.

The mean (Cntle) and anomalous (Win83e-Cntle) evaporation (E) and precipitation (P) over the North Atlantic are shown in Fig. 4. Elevated values of the mean P and E (shading) coincide with the relatively warm SSTs that extend northeastward across the North Atlantic and into the GIN and Barents Seas. Both the anomalous evaporation and precipitation are located above the ice anomalies, with reduced (enhanced) P and E over the areas with more (less) sea ice. The main exception is the negative anomaly in both P and E located just to the northeast of Iceland, well removed from any ice edge changes. Overall, the P and E anomalies are of similar magnitude and location and thus most ($\sim 72\%$) of the evaporation changes are compensated by similar changes in precipitation.

The response to the Win83e ice anomalies (Fig 5a includes both local and large-scale features. In general, the local response is prominent near the surface with anomalously low (high) SLP above reduced (enhanced) ice extent. For example, small-scale troughs are located over the eastern Greenland and western Bering Seas where the ice is reduced and a ridge is located over the Labrador Sea / southern Greenland and the Sea of Okhotsk, where the ice is more extensive than normal. One exception is that positive SLP anomalies are found above reduced sea ice extent in the Barents Sea; however, this part of the response may reflect the greater influence of the large-scale changes, which includes

positive anomalies over most of the Arctic. The large-scale response, which is more prevalent at upper levels (Fig. 5b&c), closely resembles the negative phase of North Atlantic/Arctic Oscillation, the leading pattern of variability in the control simulation (i.e. the pattern correlation between the response and the leading EOF of 500 mb height over the Northern Hemisphere in Cntle is 0.78). The large-scale response is equivalent barotropic,

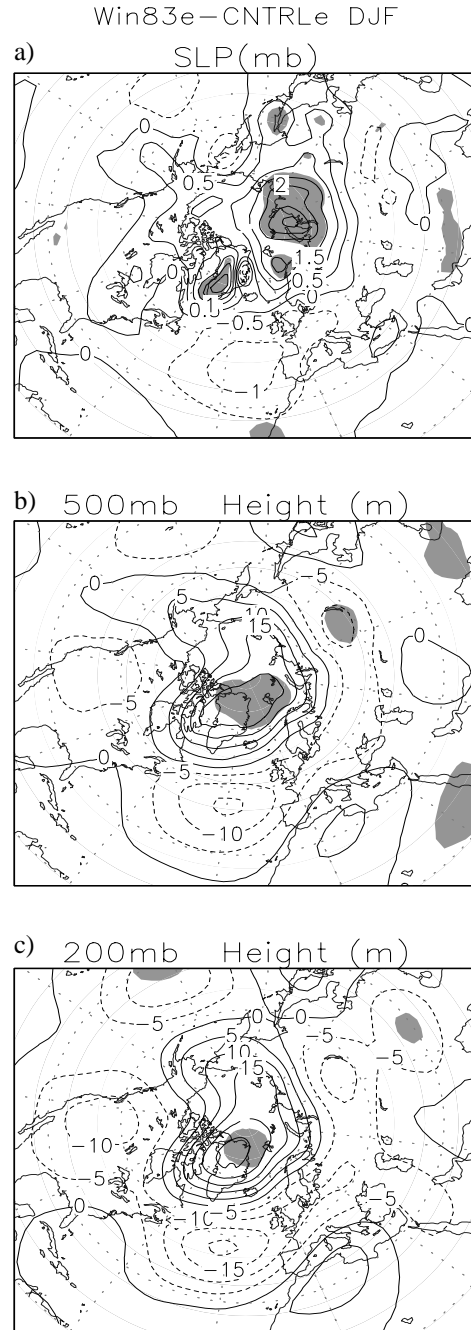


Fig. 5. Win83e anomalies (response) for (a) SLP (mb), (b) 500 mb height (m) and (c) 200 mb height (m) during DJF. The contour interval in a) is 0.5 mb and in b,c) is 5 m. The shading denotes regions where the t-statistic values exceed the 95% confidence level.

where anomalies increase in magnitude with height. The anomalies are modest with maximum amplitudes of about 15-20 (20-25) m at 500 (200) mb and only a small portion of the response is significant at the 95% level in the middle and upper troposphere.

How sensitive is the atmospheric response to the location and extent of the ice anomalies? To address this question, we compare our results to those of MDS/DMSP who also examined the CCM3 response to changes in North Atlantic ice extent derived from the observed trends over the past 40 years. The ice extent in MDS/DMSP simulations are similar to ours in that they have more ice in the Labrador Sea and less ice in the GIN and Barents Seas, but the aerial coverage is much greater in their experiments. In addition to an extended control run, MDS/DMSP performed two experiments based on the observed trend and approximately twice the trend². The anomalous ice forcing and 500 mb response from the a) Win83e, b) Trend and c) Exaggerated Trend experiments are shown in Fig. 6. The pattern of the response is very similar in all three experiments, with positive (negative) height anomalies in high (mid) latitudes, but they differ in the magnitude of the response, which increases monotonically with the extent of the ice anomalies.

The relationship between ice extent and the atmospheric response is quantified by plotting the absolute value of the monthly 500 mb anomalies versus the absolute value of the anomalous ice area, where both are averaged over the North Atlantic sector (90°W-90°E, 30°N-90°N). The values are presented in Fig. 7 for all three experiments for the months of December through April. The amplitude of the 500 mb response in all months is greatest in the Exaggerated Trend, intermediate in Trend and least in the Win83e experiment. The magnitude of the response scales nearly linearly with ice extent, i.e. the linear correlation between the two is 0.92. In addition, the y-intercept of the regression line fit to the anomalies passes within 2 m of the origin, consistent with the expectation of no response without forcing.

Comparing the simulated with observed anomalies provides some indication of how ice anomalies may be forced and/or feedback on the atmospheric circulation, with the understanding that the observed circulation anomalies result from several processes, including: internal atmospheric variability and the response to SST anomalies including those associated with El Niño/Southern Oscillation (ENSO), in addition to the response to sea ice forcing. The atmospheric circulation pattern during the winter of 1982-83 was influenced by the very strong El Niño event in the tropical Pacific. El Niño effects sea ice in the Pacific sector via a strengthening of the Aleutian low (Niebauer 1988), as occurred

in the winter of 1982-83; ENSO-induced atmospheric changes may also impact sea ice in the Atlantic sector (Gloersen 1995; Mysak et al. 1996).

The observed 500 mb height pattern during DJF of

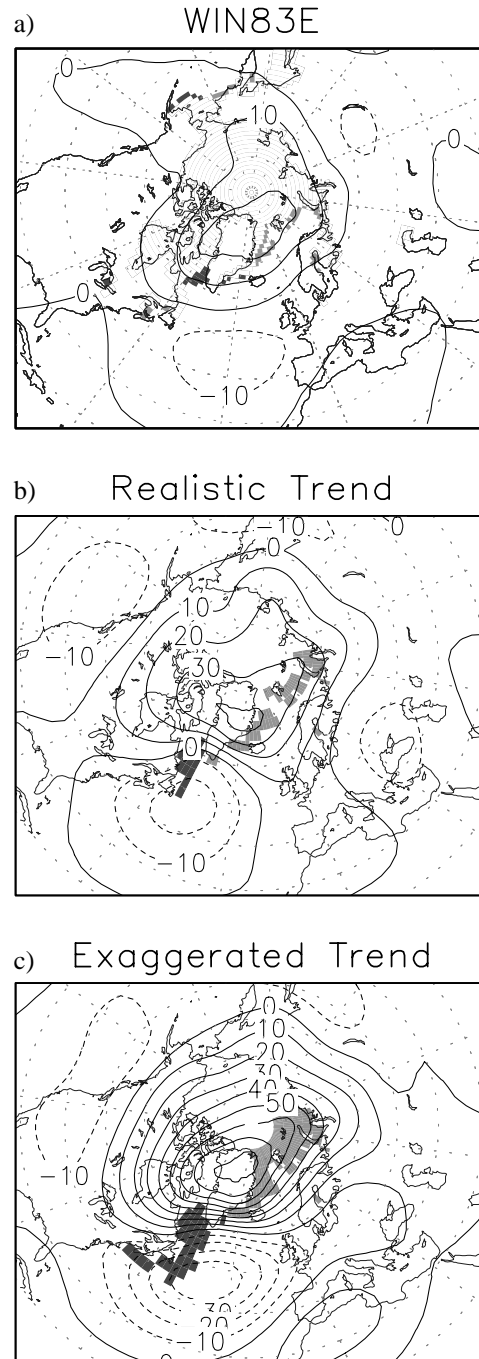


Fig. 6. The CCM response at the 500 mb level (contours) during DJF to ice anomalies (shading) in the (a) Win83e, (b) 'Realistic Trend', and (c) 'Exaggerated Trend' experiments. The contour interval is 10 m, negative contours are dashed and light (dark) shading indicate regions with less (more) ice relative to the control. The latter two experiments were recently performed by MDS/DMSP (2003), where the ice anomalies were roughly based on the observed trend and twice the trend in sea ice extent.

2. The ice extent in the realistic trend experiment is somewhat larger than the observed trend. The ice anomalies in the exaggerated ice experiment, which DMS/MDS refer to as the ice dipole experiment, are very large - on par with the change in ice cover between winter and summer.

500 mb Monthly Response in North Atlantic Sector (90W-90E, 30-90N) Dec-Apr

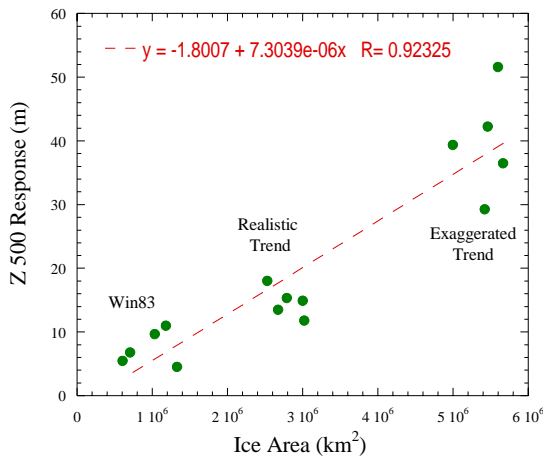


Fig. 7. Scatter plot of the magnitude of the 500 mb height anomalies versus the aerial extent of the ice anomalies averaged over the North Atlantic sector (90°W–90°E, 30°N–90°N) for the months of December through April in the Win83e, Realistic Trend and Exaggerated trend experiments. The regression line fit to the data and the correlation coefficient (R) are also shown.

1982–83 (Fig. 8) resembles the positive phase of the NAO with anomalously high (low) heights over the mid (high) latitudes. This circulation pattern, which extends to the surface (not shown), is consistent with the atmosphere forcing the ice anomalies: counter clockwise winds around the anomalous low over Greenland act to increase the ice extent in the Labrador Sea and decrease it in the GIN and Barents Seas (Deser et al. 2000, 2002). The observed 500 mb height anomaly (Fig. 8) is nearly opposite to the response of the CCM3 to the observed ice anomalies (Fig. 6a), which suggests that ice-atmosphere interactions in the North Atlantic sector damp the original atmospheric circulation anomaly, consistent with the findings of MDS/DMSP.

1983 NCEP Reanalysis

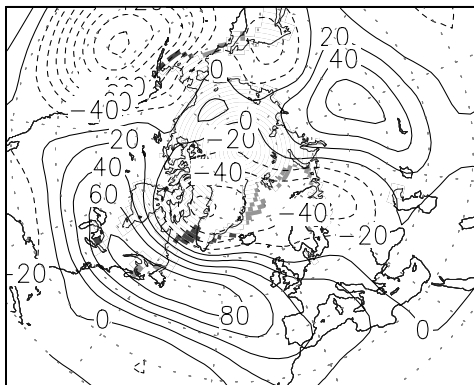


Fig. 8. Observed 500 mb height anomalies (contours) and ice anomalies (shading) during DJF of 1982–83. The contour interval is 20 m negative contours are dashed; light (dark) shading indicates less (more) ice relative to climatology.

Deser et al. (2000) examined changes in the path of storms over the North Atlantic and GIN seas based on observed storm counts during years with “low” and “high” values of the leading principal component (PC) of Arctic sea ice concentrations. Here we explore the ice-related storm track changes in the CCM and how they compare with observations, by computing the band-pass filtered near-surface meridional heat transport

(2–8 day filtered $\overline{v'T'}$ at 1000 mb) from both the National Center for Environmental Prediction (NCEP) reanalysis and from the Win83-Cntle experiment. We chose the 1000 mb level rather than 850 mbs, the traditional level for computing $\overline{v'T'}$, since the temperature perturbations are maximized in the boundary layer and decline rapidly with height (Fig. 3). By this measure, the mean storm track (shading) in the CCM (Fig9a) and reanalysis (Fig. 9b) is centered off the east coast of North America with a northeastward extension over the

GIN and Barent Seas. The difference in $\overline{v'T'}$ obtained from reanalysis between the eight low and five high ice winters used by Deser et al. (2000) has a similar ice pattern as the winter of 1982–83. We compare the model results to a composite of winter values instead of just the winter of 1982–83 to suppress the atmospheric variability unrelated to the sea ice changes.

The observed low-high composite indicates that the main part of the North Atlantic storm track is nearly doubled in strength when the ice is reduced in the GIN Seas (Fig. 9b); A similar result was found for the winter of 1982–83 Scott et al. (2003, Fig. 3). In contrast, the $\overline{v'T'}$ anomalies in the Win83e experiment indicate that there is a ~15% reduction in strength of the climatological storm track, which is part of a basin-wide dipole pattern indicative of a northwestward shift in the entire North Atlantic storm track. Like the height anomalies, the simulated storm track anomalies also suggest that the ice changes have a modest negative feedback on the strong atmospheric forcing.

On a regional scale, Deser et al. found a westward shift in the observed storm track in the GIN Seas, with an increased number of storms above reduced ice cover along much of the east coast of Greenland in the low-high composite years. A similar change in the observed-precipitation occurs for the low-high years and in the winter of 1983 (Scott et al. 2003, Fig.4). While a westward shift is also apparent in both the simulated precipi-

tation (Fig. 4b) and $\overline{v'T'}$ (Fig. 9a), the observed low-high values are of smaller scale and somewhat different locations in observations (Fig. 9b). Thus, the exact nature of the local storm track changes to the sea ice forcing is unclear from our experiments.

b) Pacific Sector: Win96e & Win83e

The ice boundary conditions in the Sea of Okhotsk during the Win83e and Win96e simulations are similar

to but less extensive than the somewhat idealized “heavy” and “light” ice conditions in the AGCM experiments performed by Honda et al. (1999). The response in their AGCM experiments, obtained from the difference between the heavy and light ice simulations, consists of a large-amplitude wave train, where the magnitude of the 500 mb height anomaly centers over Kamchatka, Alaska and Canada, exceed 150, 120 and 60 m, respectively. As a first step, we seek to confirm their findings but with more realistic ice forcing, obtained from the difference between the Win96e and

Win83e experiments averaged over DJF. The pattern of the 500 mb height anomalies (Fig. 10) is similar to the wave train found by Honda et al., with a trough over Siberia, a ridge over Alaska and a trough that extends from the eastern North Pacific to central North America. However, the anomalies are only about 10%-20% as large as those in Honda et al., with the majority of the signal resulting from the forcing in the Win96e experiment (see Figs. 5 and 12).

Several factors could contribute to the disparity between Honda et al. and our results, including differences in the boundary forcing; months used, the AGCMs employed and the ensemble size. Honda et al. used large ice anomalies (~ 2 times observations) but confined them to the Sea of Okhotsk. Thus, smaller ice anomalies north of Japan, and changes in the ice edge in other locations, especially in the Bering Sea, could impact the atmospheric circulation in our experiments relative to theirs. We also present the response in DJF while Honda et al. examined the response in JF but the response in our experiments is relatively unchanged if only JF was used. In addition, the AGCM used by Honda et al. is of lower horizontal resolution ($\sim 5.6^\circ \times 5.6^\circ$) but higher vertical resolution (30 levels) compared to the CCM3. Finally, the Honda et al. results are based on five-member ensembles compared to fifty used here. The importance of using a large ensemble becomes clear from Fig. 11, in which the 500 mb height differences (Win83e-Win96e) over the northern Sea of Okhotsk and Alaska (boxed areas in Fig. 10) are shown for all 50 pairs of simulations. The response varies widely among the simulations, with an intra-ensemble standard deviation of ~ 40 m (60 m) for the center located over the Sea of Okhotsk (Alaska). The variability among the ensemble members may be greater in the Alaskan center because it is farther downstream from the major source of the forcing.

c. The response to sea ice extent vs. ice concentration

The sea ice cover in the Win96e and Win96c experiments is reduced over most of the Atlantic and Pacific sectors of the Arctic relative to the climatological ice state in the Cntle simulation (Fig. 12). Even though the marginal ice zone, the transition region between open water and full ice cover, is compact in winter, air-sea interactions are vigorous there since surface heat fluxes are very large through leads in the ice during winter.

We examine the relationship between surface fluxes and ice fraction in a scatter diagram (Fig. 13) which shows the ensemble average of the daily sensible + latent + long wave fluxes at individual grid points as a function of ice fraction in the WIN96c experiment. Values are plotted 10 days apart in the months of November through April for all Northern Hemisphere points when the ice fraction is between 1% and 99%, since their decorrelation time scale is typically less than a week. In general, the fluxes increase as the ice fraction decreases from 99% towards completely ice free conditions and

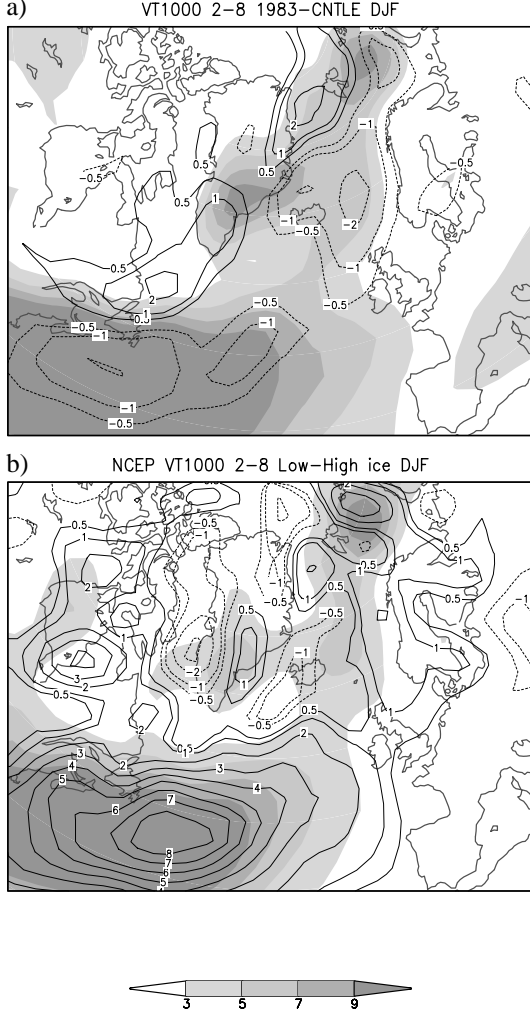


Fig. 9. The mean (shaded) and anomalous (contoured) 2-8 day band-pass filtered meridional heat transport at 1000 mb averaged over DJF from (a) the CCM and (b) reanalysis. Climatology is obtained from the long-term mean values in (a) the Cntle simulation and (b) the reanalysis over the period 1949-2000. The anomalies in (a) are from the ensemble mean Win83e-Cntle values. The anomalies in (b) are based on the leading principal component of Arctic Sea ice concentration, i.e. the composite difference between years with low (1974, 83, 84, 90, 91, 92, 93, 95) and high (1963, 66, 67, 68, 69) PC values (see Deser et al. 2000). The low-high composite has more (less) ice in the Labrador (Gin and Barents) Seas, similar to those in the Win83e experiment. The contour interval is $1 \text{ m } ^\circ\text{C sec}^{-1}$, with the $+0.5$ and -0.5 contour levels included but, the zero contour omitted. The shading interval is $2 \text{ m } ^\circ\text{C sec}^{-1}$.

Win83e–Win96e 500mb hgt(m) DJF

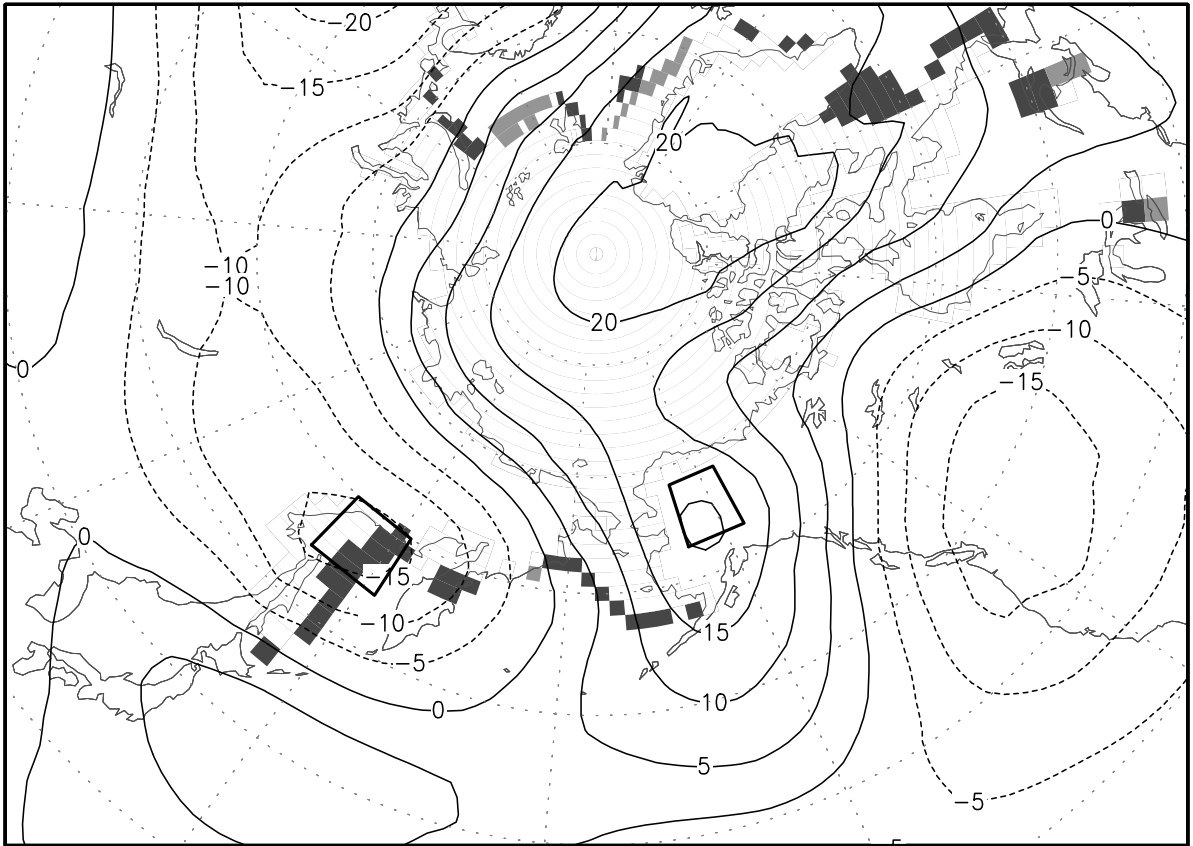


Fig. 10. The difference in 500 mb heights during DJF (contours) and ice extent during January (shading) between the Win83e and Win96e experiments. The contour interval is 5 m, negative contours are dashed; light (dark) shading indicates there is less (more) ice in the Win83e relative to the Win96e experiment. Boxes denote the regions used in Fig. 11.

this increase slows as the concentration decreases below ~50%. However, it is difficult to estimate the response curve over the entire range of ice fraction values since the spread in the flux variability is very large at medium and low ice concentrations. Additional factors such as location, wind speed and direction, etc. appear to have a much greater influence on the fluxes when the ice concentration is low. Taken as a whole, Fig. 13 suggests that an anomaly in the ice fraction would have a larger and more reproducible surface flux response if it occurs when the mean ice fraction is high than when it is low. High mean ice concentrations are prevalent in the Win96c experiment, and perhaps as a result, the surface flux anomalies are more intense and the gradient in the flux forcing across the marginal ice zone is sharper in the Win96c compared to the Win96e experiment (Scott et al. 2003, Fig. 5).

The wintertime response to the ice extent versus ice concentration anomalies is assessed by comparing the SLP and 500 mb height anomalies during DJF from the Win96e and Win96c experiments relative to the Cntle simulation (Fig. 14). The pattern of the response in the

two experiments is similar, especially at the surface. For example, in both the Win96e and Win96c experiments there are significant negative SLP anomalies over the reduced ice cover in the Sea of Okhotsk and on either side of Greenland (Fig. 12). The main difference between the experiments occurs in the free troposphere, where the 500 mb response is approximately 40–80% larger in the concentration than in the extent simulations over the Atlantic-Asian portion of the Arctic. However, the 500 mb anomalies are not amplified outside of this area, and the aforementioned wave train emanating from the Sea of Okhotsk is diminished over North America in Win96c relative to the Win96e experiment.

4. Summary and Conclusions

The purpose of this study is to better understand how realistic Arctic ice anomalies influence the atmosphere during winter; the summertime response will be examined in future work. The experimental design consists of atmospheric GCM simulations in which the sea ice boundary conditions are derived from observations. Simulations were performed for 1995–96 and 1982–83,

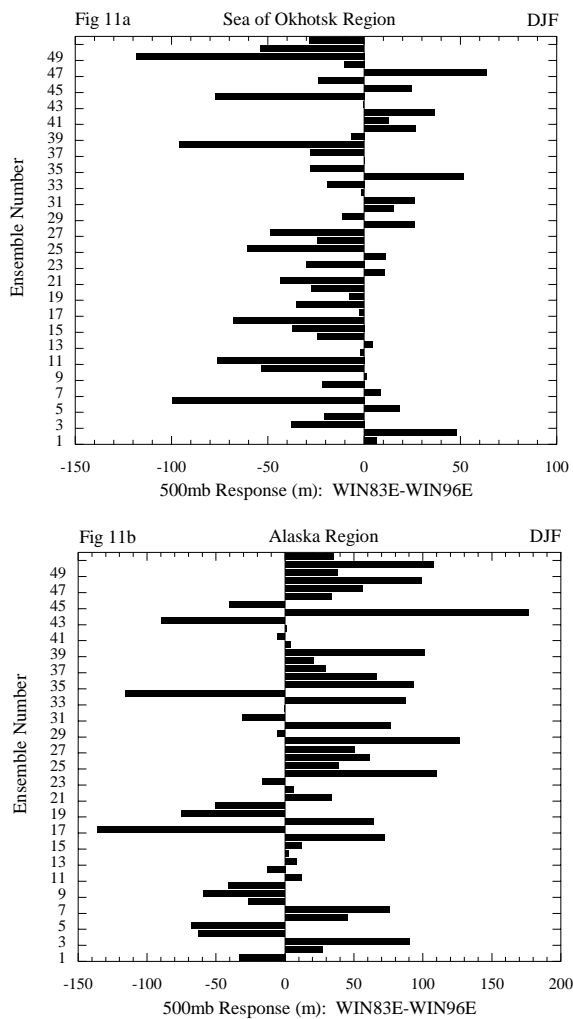


Fig. 11. The difference in the 500 mb height between the Win83e and Win96e experiments in each of the 50 ensemble members averaged over (a) the northern Sea of Okhotsk and (b) Alaskan regions shown in Fig. 10.

the winters with maximum and minimum ice coverage during 1979-99, when satellite estimates of sea ice were available. The three experiments each consist of 50 ensemble members; using large ensembles proved critical to obtaining robust results, since the internal atmospheric variability (“climate noise”) is large in mid and high latitudes of the CCM (see Fig. 11) and presumably in nature as well.

The sea ice departures in a given winter give rise to surface heat flux anomalies of relative small spatial scale (a few hundred kilometers) but very large amplitude ($> 100 \text{ W m}^{-2}$). The atmospheric response to this flux forcing can be broadly separated into a local and a remote response. The local or direct response is robust but shallow, with near-surface warming, enhanced precipitation and evaporation, and below normal sea level pressure above where the ice has receded, while the opposite occurs when the ice is more expansive. The thermal anomalies decay rapidly with height and are

Ice Boundary Cond.: Jan96

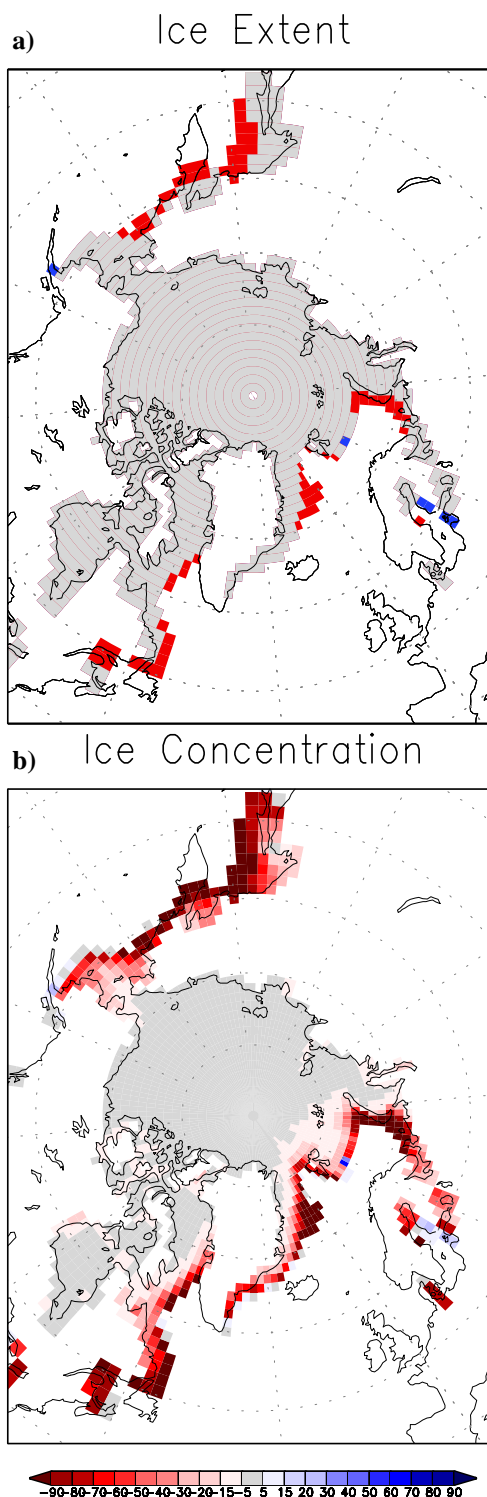


Fig. 12. Sea ice boundary conditions during January 1996 in the Win96 (a) extent and (b) concentration experiments. Gray indicates areas with climatological sea ice, blue (red) indicates grid squares with increased (reduced) ice relative to the climatology. The percent change in ice cover in Win96c relative to the Cntle simulation is given by the scale beneath panel (b).

generally confined below 700 mb. The local response is consistent with the direct linear response to a mid or high latitude boundary perturbation, resulting in a shallow heat source and baroclinic response: surface low giving way to a weak ridge aloft (e.g. see Hoskins and Karoly 1981, Saravanan 1998, Peng and Whitaker 1999; Peng and Robinson 2001)

If the ice-edge is collocated with the local storm track, as is the case in the Greenland Sea, then sea ice anomalies can influence the low-level baroclinicity and thereby impact the path and intensity of storms. In the Win83e experiment, the storm track shifts westward with the ice edge, resulting in enhanced (diminished) storm activity and precipitation over the west (east) Greenland Sea. While this is broadly consistent with the observational analyses of Deser et al. (2000), it was not possible to cleanly isolate the regional storm track response to sea ice anomalies from the large-scale response in our experiments.

The remote or large-scale response to changes in the ice depends on the interaction between the anomalous surface fluxes and the large-scale circulation. The large-scale response to reduced (enhanced) ice cover to the east (west) of Greenland weakens the main branch of the North Atlantic storm track and projects strongly on the negative phase of the AO/NAO, with a ridge over the poles and a trough at midlatitudes. While these storm track and height anomalies are consistent with each other (Lau 1988; Rogers 1990; Serreze et al. 1997), it is unclear whether the storm track changes caused or resulted from the large-scale circulation changes. Peng and Robinson (2001) and Kushnir et al. (2002), however, indicate that fluctuations in the eddy induced forcing can excite the internal modes of variability such as the AO/NAO, where interactions between the boundary driven anomalous diabatic heating and the climatological storm track result in changes in the eddy forcing. The storm track and accompanying circulation changes can be of either sign depending on the interaction between the forcing and climatological flow; here the atmospheric response is opposite to observations, suggesting a negative ice-atmosphere feedback, which is consistent with the findings of MDS/DMSP.

Sea ice anomalies in the Pacific sector generate a direct local response with characteristics similar to those in the Atlantic sector and a large-scale wave train with centers over Siberia/Sea of Okhotsk, Alaska/Arctic Ocean and western North America/eastern Pacific Ocean. Honda et al. (1999) found a similar wave train developed in response to sea ice anomalies in the Sea of Okhotsk. They attributed the large-scale response, not to changes in the storm track, which is far south of the ice edge, but to excitation of a stationary Rossby wave. The model response in their study and our extent experiments, does not resemble the dominant modes of internal variability over the Pacific, but bears considerable resemblance to observed composites of the circulation anomalies associated with minimum – maximum ice cover in the Sea of Okhotsk (Honda et al. 1996, 1999).

Thus, unlike in the Atlantic, the Pacific ice anomalies could have a positive feedback on the atmospheric circulation. However, the wave train response was less pronounced and the AO/NAO-like response more prominent in the Win96c compared to the Win96e experiment, which suggests that stronger forcing in the concentration simulations may preferentially excite internal modes of atmospheric variability.

Several factors influence the magnitude of the atmospheric response to the sea ice forcing, including the mean seasonal cycle of the ice-ocean-atmosphere system, the temporal and spatial evolution of the sea ice anomalies, and the presence of leads within the ice. Here, we mainly focused on the response to ice extent anomalies during DJF, where the magnitude of the response is modest: on the order of 2–2.5 mb at the surface and 15–20 m at 500 mb. However, a comparison of the simulations conducted here to those of MDS/DMSP, indicates that the amplitude of the response to ice anomalies in the Atlantic sector scales roughly linearly with the area of the ice anomalies. Large ice anomalies, like those that could occur due to greenhouse gas emissions, had a substantial impact (> 70 m at 500 mb) on the atmospheric circulation. The degree to which linear scaling applies to other ice configurations and models requires further study.

The wintertime response to ice concentration anomalies over the Atlantic-Asian section of the Arctic is large, in some locations twice as large, as the response to the extent anomalies. The strong impact of ice concentration changes on the response may result in part to nonlinearity in the relationship between surface heat fluxes and ice fraction (which in nature would be augmented by thinning ice), where large heat fluxes can occur through small leads but then saturate as the frac-

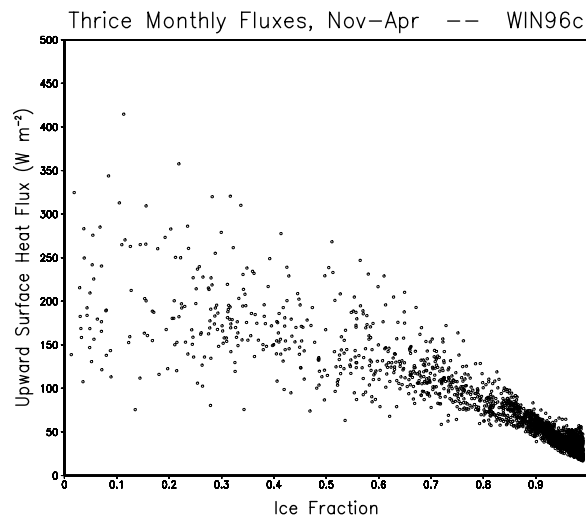


Fig. 13. Scatter plot of the ensemble average of the daily sensible + latent + long wave fluxes as a function of ice fraction at individual grid points in the Northern Hemisphere. Values are plotted on the 8th, 18th and 28th of November through April when the ice fraction is between 1% and 99%.

tion of open water increases (Ledley 1988; Simmonds and Budd 1991; Fig. 13). One important caveat is that the atmospheric response depends on how ice extent is defined. In the extent simulations performed here, the daily ice and SSTs are linearly interpolated from their monthly means of either 0% or 100% ice cover, resulting in ice concentration values at grid points where ice formed or melted in a given month, possibly reducing the difference in the atmospheric response between the extent and concentration experiments. In contrast, anomalies in both the Win96e and Win96c experiments are defined relative to the control *extent* simulation.

Thus, anomalies in the Win96c experiment include the response to the anomalous concentration and the difference in the climate between the extent and concentration simulations, which could exaggerate the influence of the change in ice fraction on the atmosphere. Nevertheless, our findings strongly suggest that changes in wintertime ice concentration has a more substantial impact on the large-scale atmospheric circulation relative to changes in ice extent, which have also been used in most previous AGCM studies.

Response to Ice Anom DJF

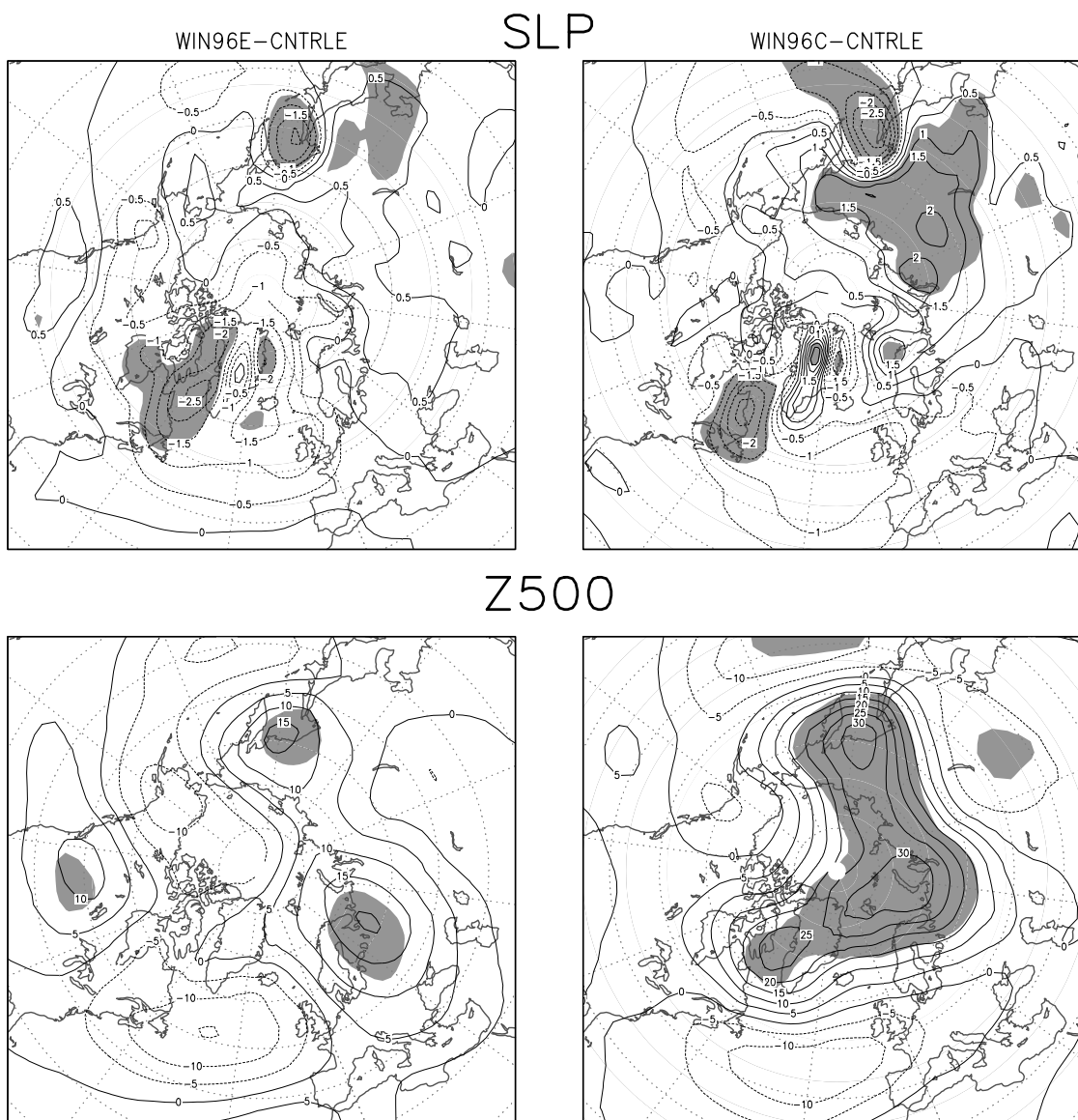


Fig. 14. The SLP (top) and 500 mb height (bottom) anomalies in the Win96e (left) and Win96c experiments during DJF. The SLP (height) contour interval is 0.5 mb (5m), negative contours are dashed and shading denotes regions where the t-statistic values exceed the 95% confidence level.

Acknowledgements. We thank Clara Deser, Gudrun Magnúsdóttir and R. Saravanan for providing us the output from their model simulations and their suggestions on improving the manuscript. We also thank Steve Worley at NCAR for providing the HadISST data set. This research was supported by a grant from the NOAA's Arctic Research Office issued through the International Arctic Research Center (IARC). USB was supported by the Frontier Research System for Global change through IARC. The model simulations were performed at the Arctic Regional Supercomputer Center; we thank Guy Robinson for his assistance with supercomputing issues.

References

- Agnew, T., 1993: Simultaneous winter sea-ice and atmospheric circulation anomaly patterns. *Atmos. Ocean*, **31**, 259-280.
- Bitz, C., J. C. Fyfe, and G. M. Flato, 2002: Sea ice response to wind forcing from AMIP models. *J. Climate*, **15**, 522-536.
- Cavaleri, D. J. and C. L. Parkinson, 1987: On the relationship between atmospheric circulation and fluctuations in sea ice extents of the Bering and Okhotsk seas. *J. Geophys. Res.*, **92**, 7141-7162.
- Chapman, W. L., and J. E. Walsh, 1993: Recent variations of sea ice and air-temperature in high-latitudes. *Bull. Amer. Met. Soc.*, **74**, 33-47.
- Deser, C., J. E. Walsh, and M. S. Timlin, 2000: Arctic sea ice variability in the context of recent atmospheric circulation trends. *J. Climate*, **13**, 617-633.
- Deser, C., M. Holland, G. Riverdin, and M. Timlin, 2002: Decadal variations in Labrador Sea ice cover and North Atlantic sea surface temperatures. *J. Geophys. Res.*, **107**, 10.1029/2000JC000683.
- Deser, C., G. Magnúsdóttir, R. Saravanan, and A. Phillips, 2003: The effect of North Atlantic SST and sea ice anomalies on the winter circulation in CCM3. Part II: Direct and indirect components of the response. *J. Climate*, submitted.
- Dickson, R. R., J. Meincke, S. A. Malmberg, and A. J. Lee, 1988: The "great salinity anomaly" in the northern North Atlantic 1968-1982. *Prog. Oceanogr.*, **20**, 103-151.
- Fang, Z. and J. M. Wallace, 1994: Arctic sea ice variability on a timescale of weeks: Its relation to atmospheric forcing. *J. Climate*, **7**, 1897-1913.
- Gates, L. W. and collaborators, 1999: An overview of the results of the Atmospheric Model Intercomparison Project (AMIP I). *Bull. Amer. Met. Soc.*, **80**, 29-55.
- Gloersen, P., 1995: Modulation of sea ice cover by ENSO events. *Nature*, **373**, 503-506.
- Goosse, H., F. M. Selten, R. J. Haarsma, and J. D. Opsteegh, 2002: A mechanism of decadal variability of the sea-ice volume in the Northern Hemisphere. *Climate Dynamics*, **19**, 61-83.
- Hack, J. J., J. T. Kiehl, and J. W. Hurrell, 1998: The hydrologic and thermodynamic characteristics of the NCAR CCM3. *J. Climate*, **11**, 1151-1178.
- Herman, G. T. and W. T. Johnson, 1978: The sensitivity of the general circulation of arctic sea ice boundaries: a numerical experiment. *Mon. Wea. Rev.*, **106**, 1649-1664.
- Honda, M., K. Yamazaki, Y. Tachibana, and K. Takeuchi, 1996: Influence of Okhotsk sea ice extent on the atmospheric circulation. *Geophys. Res. Lett.*, **23**, 3595-3598.
- Honda, M., K. Yamazaki, H. Nakamura, and K. Takeuchi, 1999: Dynamic and thermodynamic characteristics of the atmospheric response to anomalous sea-ice extent in the Sea of Okhotsk. *J. Climate*, **12**, 3347-3358.
- Hoskins, B. J. and D. J. Karoly, 1981: The steady linear response of a spherical atmosphere to thermal and orographic forcing. *J. Atmos. Sci.*, **38**, 1179-1196.
- Hurrell, J. W., Y. Kushnir, G. Ottersen, M. Visbeck, Eds., 2003: *The North Atlantic Oscillation: Climate Significance and Environmental Impact*. Vol. 134. *Geophysical Monograph Series*, American Geophysical Union, 279 pp.
- Hurrell, J. W., J. J. Hack, B. A. Boville, D. L. Williamson, and P. J. Rasch, 1998: The dynamical simulation of the NCAR Community Climate Model version3. *J. Climate*, **11**, 1207-1236.
- Ikeda, M., 1990: Decadal oscillations of the air-ice-ocean system in the Northern Hemisphere. *Atmos. Ocean*, **28**, 106-139.
- Ikeda, M., J. Wang, and J.-P. Zhao, 2001: Hypersensitive decadal oscillations in the Arctic/subarctic Climate. *Geophys. Res. Lett.*, **28**, 1275-1278.
- Kiehl, J. T., J. J. Hack, G. B. Bonan, B. A. Boville, and P. J. Rasch, 1998: The National Center for Atmospheric Research Community Climate Model: CCM3. *J. Climate*, **11**, 1131-1149.
- Kushnir, Y., W. A. Robinson, I. Bladé, N. M. J. Hall, S. Peng, and R. Sutton, 2002: Atmospheric response to extratropical SST anomalies: Synthesis and evaluation. *J. Climate*, **15**, 2205-2231.
- Lau, N., C., 1988: Variability of the observed midlatitude storm tracks in relation to low-frequency changes in the circulation pattern. *J. Atmos. Sci.*, **45**, 2718-2743.
- Ledley, T. S., 1988: For a lead-temperature feedback in climate variation. *Geophys. Res. Lett.*, **15**, 36-39.
- Magnúsdóttir, G., C. Deser, and R. Saravanan, 2003: The effect of North Atlantic SST and sea ice anomalies on the winter circulation in CCM3. Part I: Main features of the response. *J. Climate*, submitted.
- Murray, R. J. and I. Simmonds, 1995: Responses of climate and cyclones to reductions in Arctic sea ice. *J. Geophys. Res.*, **100**, 4791-4806.
- Mysak, L. A. and D. K. Manak, 1989: Arctic sea ice extent and anomalies, 1953-1984. *Atmos. Ocean*, **27**, 376-405.
- Mysak, L. A. and S. A. Venegas, 1998: Decadal climate oscillations in the Arctic: A new feedback loop for atmosphere-ice-ocean interactions. *Geophys. Res. Lett.*, **25**, 3607-3610.
- Mysak, L. A., D. K. Manak, and R. F. Marsden, 1990: Sea-ice anomalies in the Greenland and Labrador Seas during 1901-1984 and their relation to an interdecadal Arctic climate cycle. *Climate Dyn.*, **5**, 111-133.
- Mysak, L. A., R. G. Ingram, J. Wang, and A. V. D. Baaren, 1996: The anomalous sea-ice extent in Hudson Bay, Baffin Bay and the Labrador Sea during three simultaneous ENSO and NAO episodes. *Atmos. Ocean*, **34**, 313-343.

- Newson, R. L., 1973: Response of a general circulation model of the atmosphere to the removal of the Arctic ice cap. *Nature*, **241**, 39-40.
- Niebauer, H. J., 1988: Effects of El Niño-Southern Oscillation and North Pacific Weather patterns on interannual variability in the southern Bering Sea. *J. Geophys. Res.*, **93**, 5051-5068.
- Parkinson, C. L., D. Rind, R. J. Healy, and D. G. Martinson, 2001: The impact of sea ice concentration on climate model simulations with the GISS GCM. *J. Climate*, **14**, 2606-2623.
- Parkinson, C. L., D. J. Cavalieri, P. Gloersen, H. J. Zwally, and J. Comiso, 1999: Arctic sea ice extents, areas and trends, 1978-1996. *J. Geophys. Res.*, **104**, 20,837-20,856.
- Peng, S. and J. S. Whitaker, 1999: Mechanisms determining the atmospheric response to midlatitude SST anomalies. *J. Climate*, **12**, 1393-1408.
- Peng, S. and W. A. Robinson, 2001: Relationships between atmospheric internal variability and the responses to an extratropical SST anomaly. *J. Climate*, **14**, 2943-2959.
- Polyakov, I. V. and M. A. Johnson, 2000: Arctic decadal and interdecadal variability. *Geophys. Res. Lett.*, **27**, 4097-4100.
- Proshutinsky, A. Y. and M. A. Johnson, 1997: Two circulation regimes of the wind driven Arctic Ocean. *J. Geophys. Res.*, **102**, 12,493-12,514.
- Randall, D., Curry J, Battisti D, Flato G, Grumbine R, Hakkinen S, Martinson D, Preller R, Walsh J, and W. J., 1998: Status of and outlook for large-scale modeling of atmosphere-ice-ocean interactions in the Arctic. *Bull. Amer. Met. Soc.*, **79**, 197-219.
- Raymo, M. E., D. Rind, and W. F. Ruddiman, 1990: Climatic effects of reduced Arctic sea ice limits in the GISS II general circulation model. *Paleoceanography*, **5**, 367-382.
- Rayner, N. A., D. E. Parker, P. Frich, E. B. Horton, C. K. Folland, and L. V. Alexander, 2000: SST and sea ice fields for ERA40. *Proceedings of the second WCRP International Conference on Reanalysis*, Reading, England.
- Robertson, A. W., M. Ghil, and M. Latif, 2000: Interdecadal changes in atmospheric low-frequency variability with and without boundary forcing. *J. Atmos. Sci.*, **57**, 1132-1140.
- Rodwell, M. J., D. P. Rowell, and C. K. Folland, 1999: Oceanic forcing of the wintertime North Atlantic Oscillation and European climate. *Nature*, **398**, 320-323.
- Rogers, J. C., 1981: Spatial variability of seasonal sea-level pressure and 500 hPa height anomalies. *Mon. Wea. Rev.*, **109**, 2093-2105.
- , 1990: Patterns of low-frequency monthly sea level pressure (1899-1986) and associated cyclone frequencies. *J. Climate*, **3**, 1364-1379.
- Royer, J. F., S. Planton, and M. Deque, 1990: A sensitivity experiment for the removal of Arctic sea ice with the French spectral general circulation model. *Climate Dynamics*, **5**, 1-17.
- Sardeshmukh, P. D., G. P. Compo, and C. Penland, 2000: Changes of probability associated with El Niño. *J. Climate*, **13**, 4268-4286.
- Scott, J. D., M. A. Alexander, M. S. Timlin, U. S. Bhatt, J. Miller, and J. E. Walsh, 2003: CCM3 sea ice forcing experiments: Boundary conditions and response in winter. [Available online from <http://www.cdc.noaa.gov/~jds/Ice/>]
- Serreze, M. C., F. Carse, R. G. Barry, and J. C. Rogers, 1997: Icelandic low cyclone activity: Climatological features, linkages with the NAO, and relationships with recent changes in the Northern Hemisphere circulation. *J. Climate*, **10**, 453-464.
- Serreze, M., J. E. Walsh, F. S. Chapin, T. Osterkamp, M. Dyurgerov, V. Romanovsky, W. C. Oechel, J. Morison, T. Zhang, and R. G. Barry, 2000: Observational evidence of recent change in the northern high-latitude environment. *Climatic Change*, **46**, 159-207.
- Simmonds, I. and W. F. Budd, 1991: Sensitivity of the southern hemisphere circulation to leads in the Antarctic pack ice. *Quart. J. Roy. Meteor. Soc.*, **117**, 1003-1024.
- Slonosky, V. C., L. A. Mysak, and J. Derome, 1997: Linking arctic sea ice and atmospheric circulation anomalies on interannual and decadal timescales. *Atmos.-Ocean*, **35**, 333-366.
- Walsh, J. E., 1983: Role of sea ice in climate variability: theories and evidence. *Atmos.-Ocean*, **21**, 229-242.
- Walsh, J. E. and C. M. Johnson, 1979: An analysis of Arctic sea ice fluctuations, 1953-77. *J. Phys. Oceanogr.*, **9**, 580-591.
- Walsh, J. E. and H. J. Zwally, 1990: Multiyear sea ice in the arctic: model and satellite-derived. *J. Geophys. Res.*, **11**, 11,613-11,628.
- Warshaw, M. and R. R. Rapp, 1973: An experiment on the sensitivity of a global circulation model. *J. Appl. Meteor.*, **12**, 43-49.
- Weatherly, J. W., B. P. Briegleb, W. G. Large, and J. A. Maslanik, 1998: Sea ice and polar climate in the NCAR CSM. *J. Climate*, **11**, 1472-1486.
- Williams, J., R. G. Barry, and W. Washington, 1974: Simulation of the atmospheric circulation using the NCAR global circulation model with ice age boundary conditions. *J. Appl. Meteor.*, **13**, 305-317.